LA-UR-81-3728

MASTER

CONF-820209--1

LA-UR--81-3728

DE82 006133

TITLE: NERVE-PULSE INTERACTIONS

AUTHOR(S): Alwyn C. Scott

SUBMITTED TO: U. S. - Japan Seminar on Competition and Cooperation in Neural Nets, Kyoto, Japan, February 15-19, 1982

DISTRIBUTION OF THIS DOCUMENT IS UNLIMITED

# Los Alamos
Los Alamos National Laboratory
Los Alamos, New Mexico 87545

# NERVE PULSE INTERACTIONS

Alwyn C. Scott
Center for Nonlinear Studies
Los Alamos National Laboratories
Los Alamos, New Mexico   87545   USA

## INTRODUCTION

Traditionally the neuron has been viewed as a linear threshold unit which generates an output when some weighted sum of the inputs exceeds a certain value. Over the past two decades, however, several suggestions have been made for mechanisms by which the neuron might perform more sophisticated forms of information processing, such as: Boolean logic at dendritic branches [1-8], Time code to space code translations on the axonal tree [9-14], and Dendrodendritic interactions [15]. Such suggestions have led Waxman to propse the concept of a "multiplex neuron" [16] which bears about the same relationship to a linear threshold unit as does a "chip" to a "gate" in modern integrated circuit technology.

Certainly au important aim of neuroscience is to understand the true functional roles played by neurons. A first step in this direction is to ask what it is that a neuron can do. This is a question of biophysics. From this spectrum of possible modes of neuronic behavior, one can then ask the biological question: What is it that a particular neuron does do?

Here I review some recent experimental and theoretical results on mechanisms through which individual nerve pulses can interact. Three modes of interactions are considered: 1) Interaction of pulses as they travel along a single fiber which leads to velocity dispersion, 2) Propagation of pairs of pulses through a branching region leading to quantum pulse code transformations, and 3) Interaction of pulses on parallel fibers through which they may form a pulse assembly. This notion is analogous to Hebb's concept of a "cell assembly" [17], but on a lower level of the neural hierarchy. It may help to explain the extreme sensitivity of neural systems to nonionizing electromagnetic fields [18,19].

## VELOCITY DISPERSION

Consider the "twin pulse" experiment sketched in Fig. 1. The times $t_1$ and $t_3$ are when the first and second pulses, respectively, pass the first electrode. The time $t_2$ and $t_4$ are similarly related to the second electrode. Thus the average
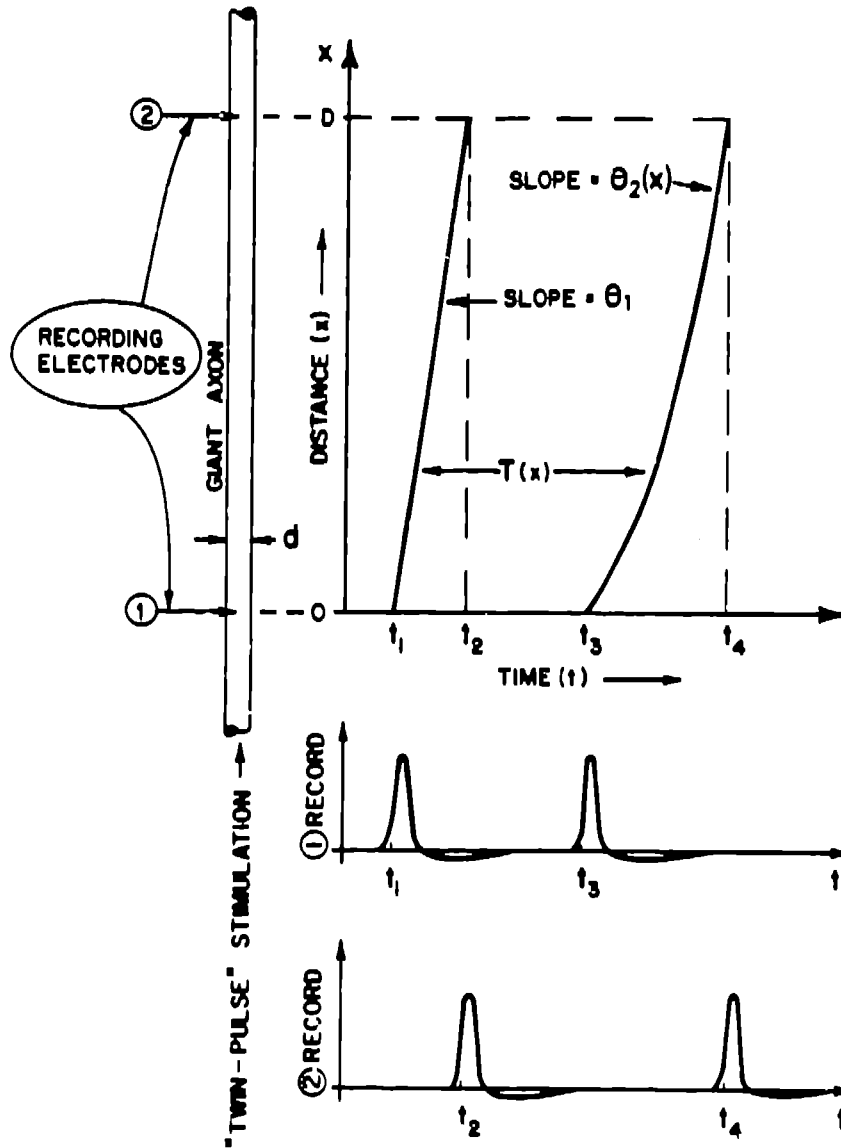
Fig. 1. Experimental details of
twin pulse experiment on giant axon of squid.

time interval between the two pulses is measured as

$$T = \frac{1}{2}(t_4 + t_3 - t_2 - t_1) , \tag{1}$$

and the ratio of the speed of the second pulse, $\theta_2$, to that of the first pulse, $\theta_1$, is

$$R = \theta_2/\theta_1$$

$$= \frac{t_2 - t_1}{t_4 - t_3} . \tag{2}$$

Actually (2) is not exact because the speed of the second pulse is not constant. A small correction to account for this effect is discussed in [20]. Since the time

differences for a squid giant axon are a few milliseconds and can be measured with an rms accuracy of about 0.003 milliseconds, (1) and (2) determine the velocity dispersion function, R(T), with an accuracy of a few per cent.

A calculation of R(T) can be made by noting that the leading edge of the second pulse propagates into the tail of the first pulse. Since all parameters that describe the axon are identical for the two pulses, the velocity dispersion function is readily calculated as (see [20] for details)

$$R(T) = \left[ \frac{1 + K}{\left(1 - \frac{V(T)}{V_T}\right) 1 + K\left[\left(\frac{1 - V(T)/V_T}{1 + V(T)/V_+}\right)\right]} \right]^{\frac{1}{2}} \tag{3}$$

where $V_T$ is the threshold voltage of an isolated pulse, and $V_+$ and $V(T)$ describe the tail of an isolated pulse as is indicated in Fig. 2.
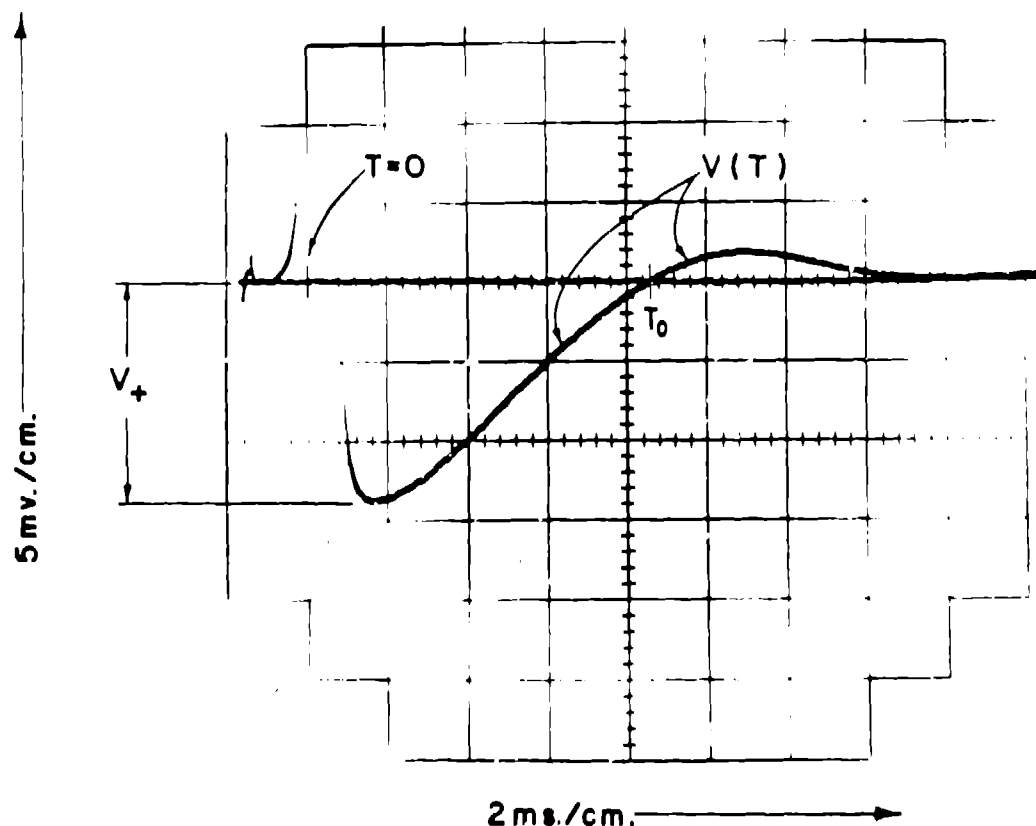


Fig. 2. The tail of a typical isolated pulse on a squid giant axon. The time T = 0 indicates when the pulse voltage passes through threshold (dv/dT = maximum value).

In (3) the parameter

$$K \equiv g_o \, \tau/c \qquad\qquad\qquad\qquad (4)$$

where $\tau$ is the time constant for exponential rise of the leading edge below threshold and $c/g_o$ is the time constant of a resting membrane (= 1 millisecond).

In Fig. 3 a measurement of $R(T)$, from (1) and (2), is compared with calculations from (3). There are four calculations because the tail of an isolated pulse was measured on both electrodes before and after the measurements of $R(T)$.

The measurements displayed in Fig. 3 confirm previous measurements by Donati and Kunov [21] and are in agreement with recent numerical studies of the Hodgkin-Huxley equations by Miller and Rinzel [22]. Particularly interesting is the "overshoot" when $R < 1$ and the second pulse is actually going faster than the first.

From the measurements one can define $T_1$ as the pulse spacing at which $R(T)$, determined from (1) and (2), is equal to unity   Likewise from the calculations one can define $T_o$ as the pulse spacing at which $R(T)$, determined from (3), is equal to unity.  In Fig. 4 a comparison of $T_1$ with $T_o$ is presented for
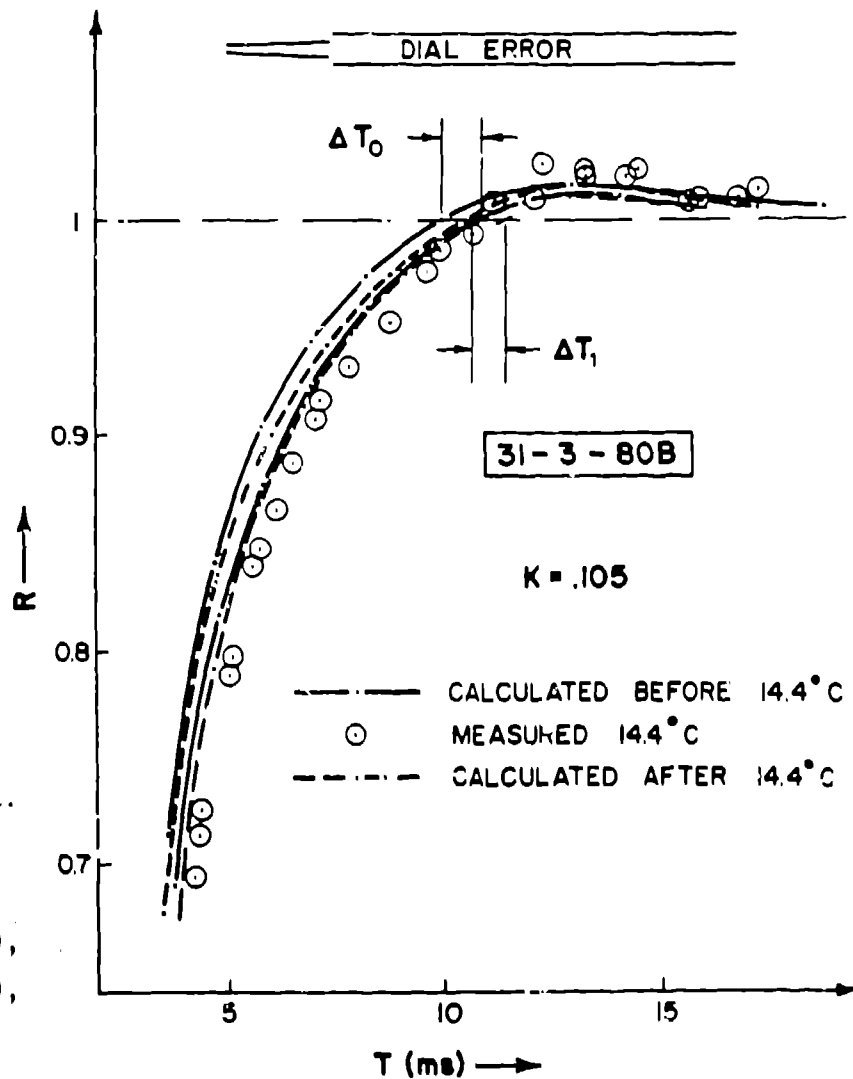


Fig. 3.   Comparison of measurements and calculations of the velocity dispersion function $R(T)$.

measurements on twelve giant squid axons where the error bars are defined as indi-
cated on Fig. 3.  Figure 4 indicates

$$T_1 \doteq T_0 \qquad (5)$$

within the accuracy of the measurements and calculations.  However (3) implies that
$T_0$ is the time at which
the tail crosses through
zero; i.e., $V(T_0) = 0$ (see
also Fig. 2).  However cal-
culations by John Rinzel
for the Hodgkin-Huxley equa-
tions do rot confirm this
point.  He finds [23]

| Temp (°C) | $T_1$ (ms.) | $T_0$ (ms.) |
|-----------|-------------|-------------|
| 18.5      | 4.77        | 6.14        |
| 14.0      | 7.25        | 8.53        |
| 6.3       | 16.0        | 17.2        |

These calculations are plot-
ted as "⊙" on Fig. 4 and
appear to lie below the
experimental data although
this distinction is not
quite clear.  This dis-
crepancy may arise because
the Hodgkin-Huxley equations
do not account for potassium
build up in the periaxonal
space [24 25].
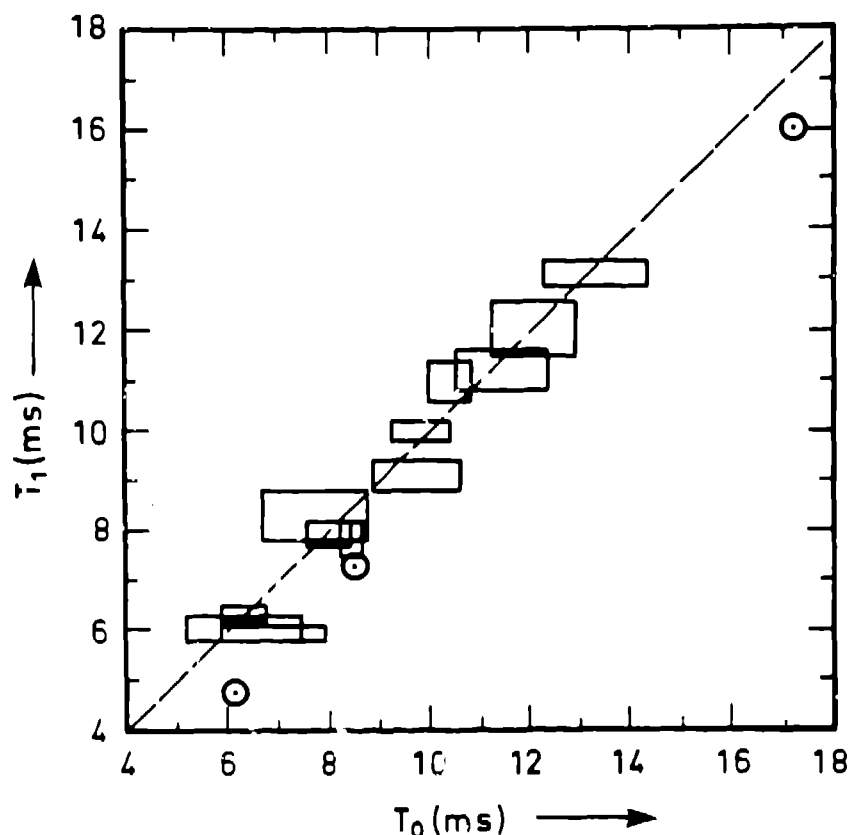


Fig. 4.  Comparison of measured $T_1$ and calculated
$T_0$ for twelve giant squid axons.  The points ⊙ are
calculated [23] from the Hodgkin-Huxley equations.

Apart from theoretical descriptions, it is interesting to consider all the
measurements of R vs T normalized to $T_1$ (made at the Stazione Zoologica between
January and June of 1980) on the "flyspeck" diagram of Fig. 5.  Within a few per
cent, the data of Fig. 5 can he represented by the empirical relation

$$R = 1 + 0.105 \left[ \frac{T}{T_1} - 1 \right] \exp \left[ 2.4 \left( 1 - \frac{T}{T_1} \right) \right]. \qquad (6)$$

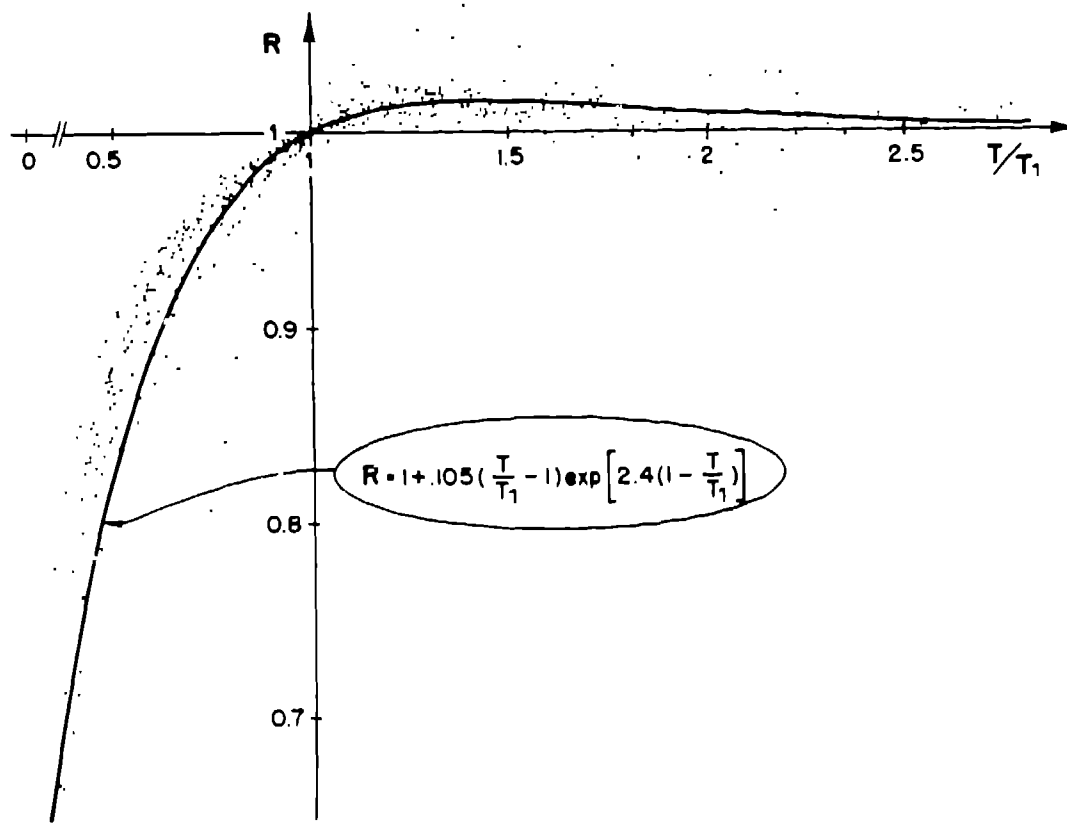Fig. 5. Measured values of R vs $T/T_1$. Note that $T_1$ is defined such that $R(T_1) = 1$.

It should perhaps be emphasized that the velocity dispersion implied by (6) is not a negligible effect. The measurements displayed in Fig. 6, for example, show considerable "frequency smoothing" between the upstream record A and the downstream
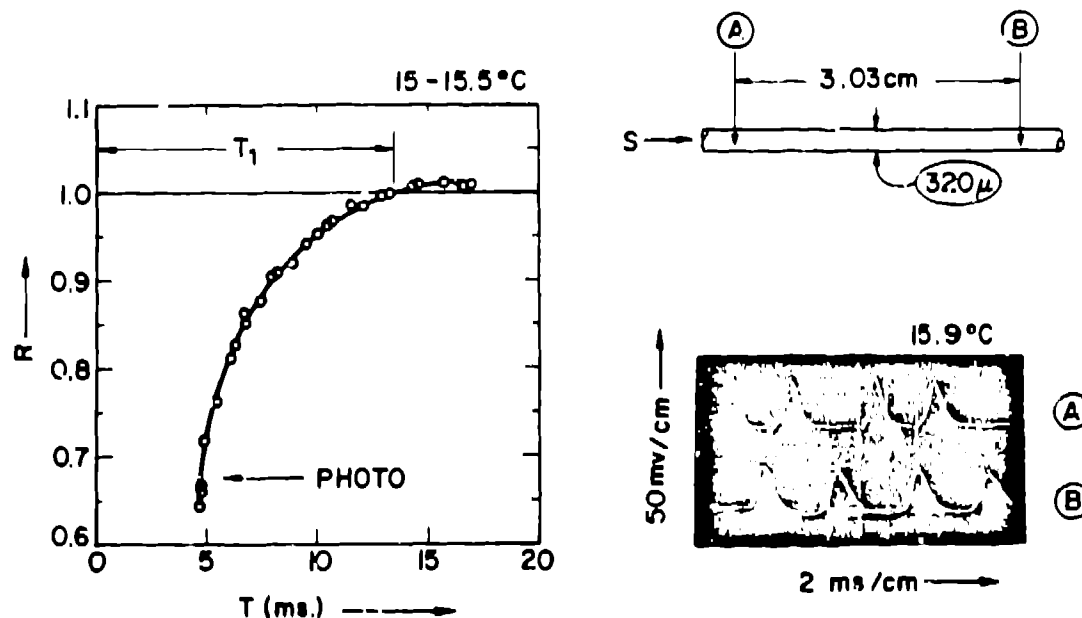


Fig. 6. Frequency smoothing on a squid giant axon.

## QUANTUM PULSE CODE TRANSFORMATIONS

We turn now to experimental situations in which a nerve pulse disappears suddenly during the course of its propagation.  I term such effects "quantum" pulse code transformations to distinguish them from differential transformations related to velocity dispersion.  An obvious place to seek quantum transformations is at the points where fibers branch (or "bifurcate").  Branches of the squid giant axon are found at the locations indicated in Fig. 7.
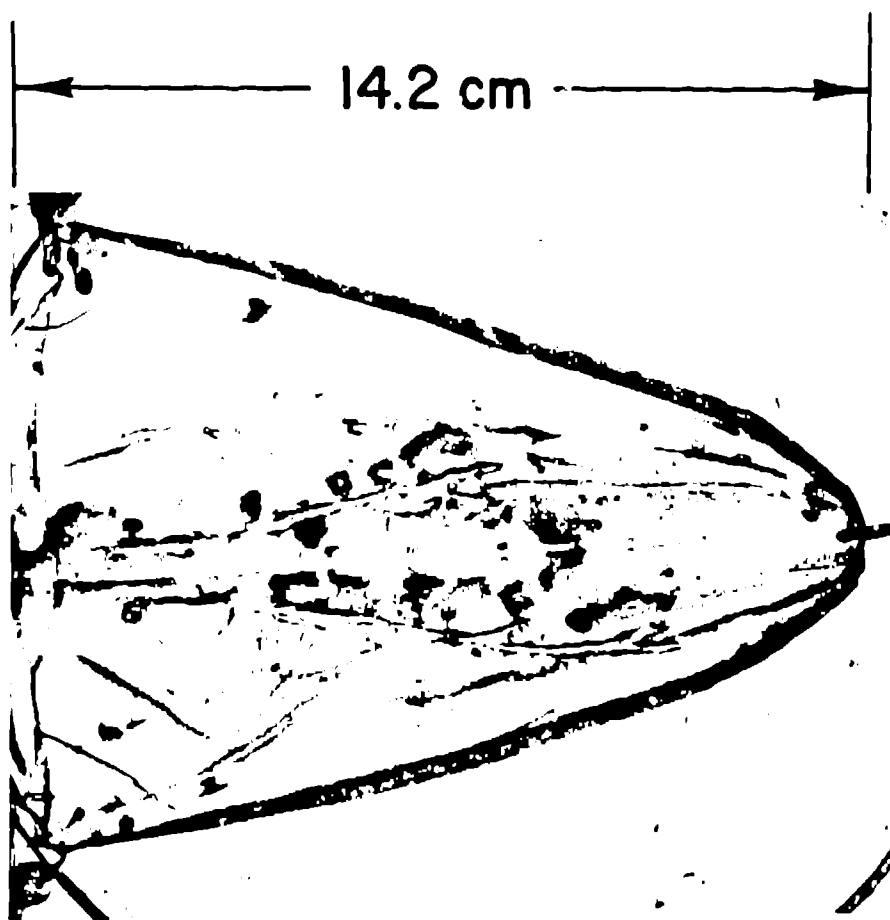


Fig. 7.  Mantle of squid (Loligo vulgaris) showing scars where giant axons and branches have been removed.

Some typical branches of the squid giant axon are displayed in Fig. 8 from which a large variation in the ratios of fiber diameters is observed.  A measure of the difficulty experienced by a pulse as it propagates through a branching region is expressed by the geometrical ratio (GR) [26] which is essentially the total characteristic admittance of outgoing fibers divided by that carrying the incoming pulse.  In terms of fiber diameters (d) it takes the form

19-5-80B        5-5-80A        6-5-80A

500μ

25-5-80A        28-5-80C        7-5-80B

Fig. 8. Typical branches of squid giant axon.

$$GR = \frac{\sum d_{out}^{3/2}}{d_{in}^{3/2}} .$$

(7)

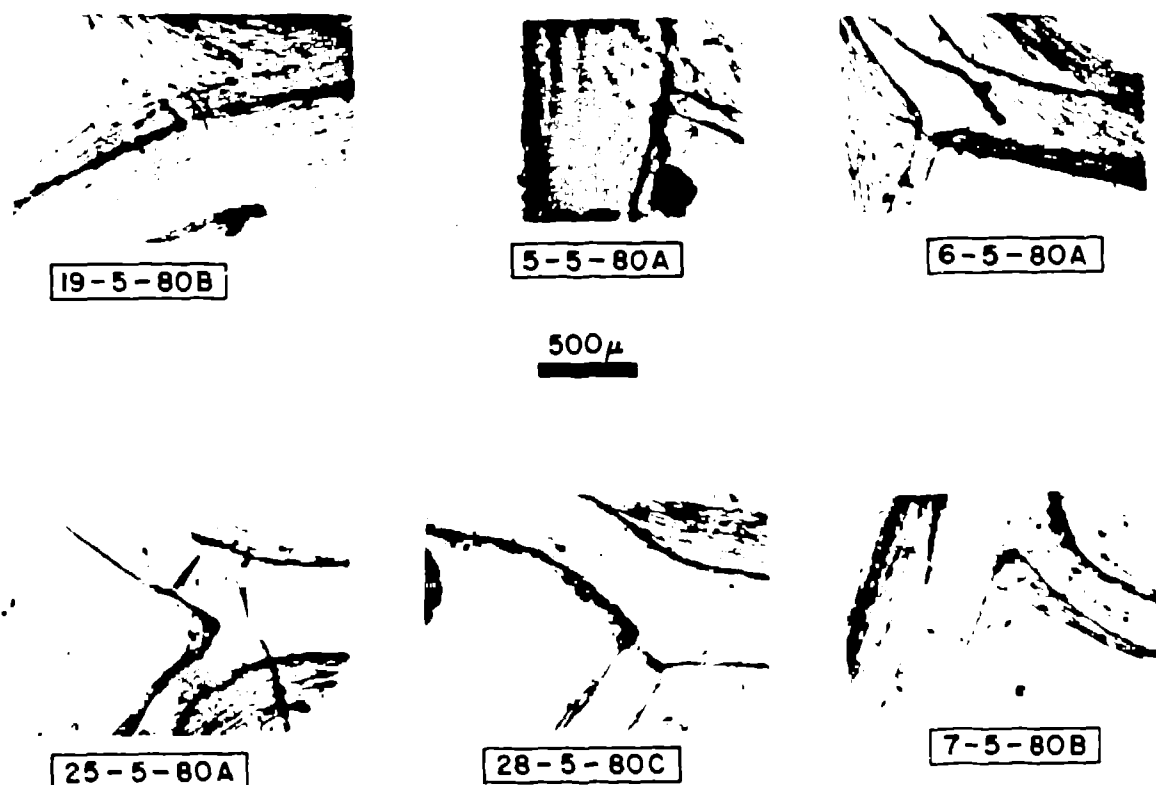If GR = 1, the "impedance matching" between outgoing and incoming fibers is perfect and a pulse proceeds through the branch with a minimum of difficulty. As GR becomes progressively greater than one, difficulties increase. Numerical calculations based on the Hodgkin-Hyxley model axon indicate that a solitary pulse will fail to propagate though a bifurcation with GR greater than about 10 [27,28].

A histogram for the GR's observed on branchings of squid giant axons under the assumption of orthodromic stimulation (i.e. incoming pulse on the main fiber) is presented in Fig. 9. It should be emphasized that these bifurcations include rather equal representations of all the different diameter ratios shown in Fig. 8; thus it seems that in the squid (Loligo vulgaris) nature is attempting to match impedences

for orthodromic conduction under a variety of geometrical constraints. I have carefully examined sixteen bifurcations under orthodromic stimulation seeking evidence for a quantum change in a temporal pulse code before and after the bifurcation. Although such a change was sometimes observed, I failed to find any case for which surgical damage or the effects of tiring the axon during the search could be eliminated. This is consistent with the observations reported in Refs. [13 and 14].

It is interesting, therefore, to turn to antidromic stimulation where the incoming pulse is on one of the daughter branches and geometrical ratios greater than unity are readily



Fig. 9. Histogram of orthodromic GR's for 109 branches of the squid giant axon.

obtained. A typical example is bifurcation #20-3-80A which is shown in Fig. 10. With stimulation (as shown) on the 340 micron daughter, the GR = 1.71. In Fig. 10b are displayed the records of a single pulse on both the upstream electrode (B) and the downstream electrode (A). Figure 11 shows that upon stimulation of #20-3-80A with a pulse rate of 160 pps. in a single burst of one half second, I observed a gradual change in the outgoing pulse train until, after 200 milliseconds, the output pulse rate was 80 pps. This effect was observed on several preparations and, for a particular preparation was quite stable and reproducible. It is likely that the mechanism here is related to potassium accumulation in the periaxonal space [13,14,24,25,29].

An example that demonstrates the failure of two pulses to propagate through a branch is shown for #29-2-80B in Figs. 12 and 13. From Fig. 12a the GR = 2.14 and the state of health for isolated pulses is displayed in Fig. 12b. Figure 13 shows a critical value of pulse interval at which the second pulse just fails (upper) or
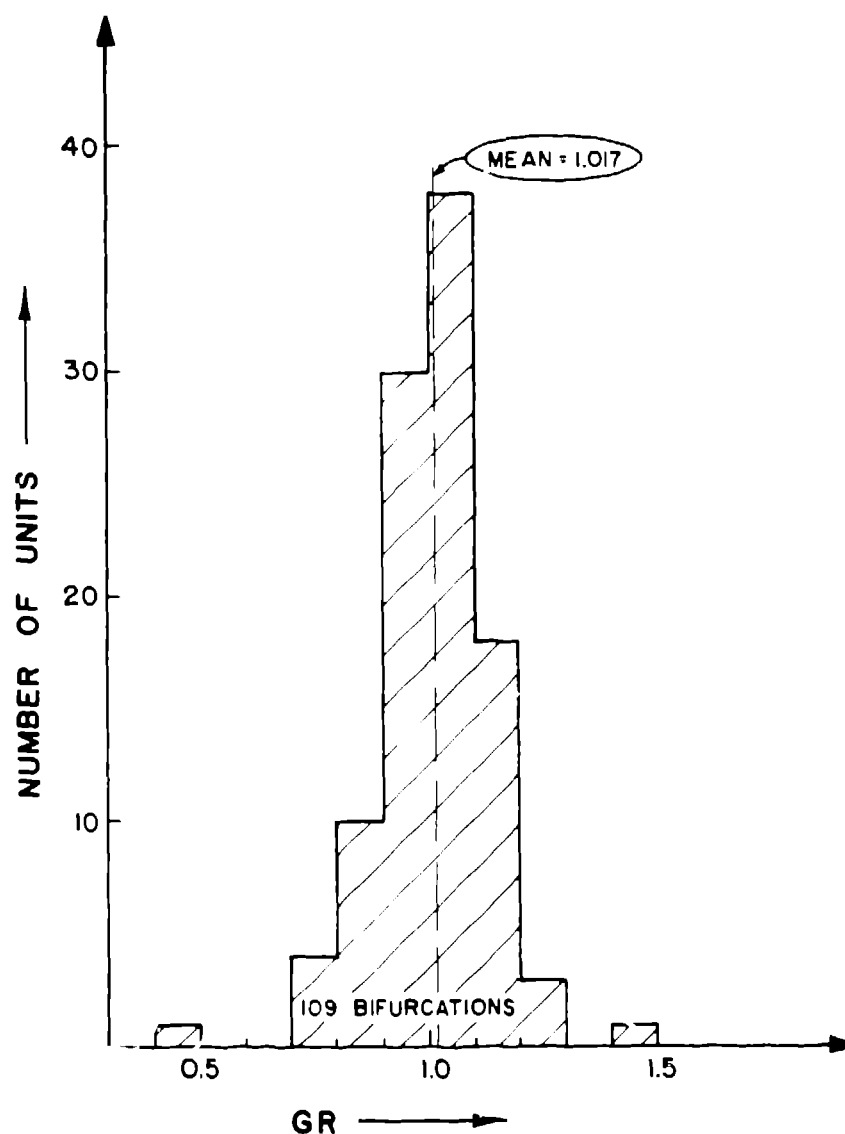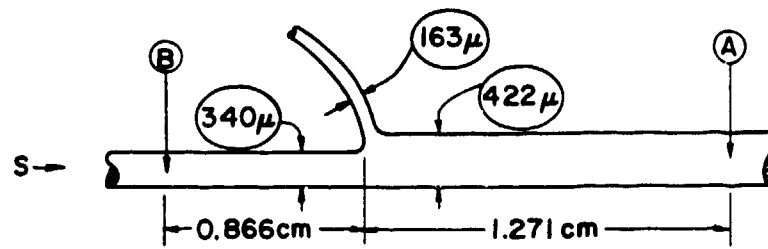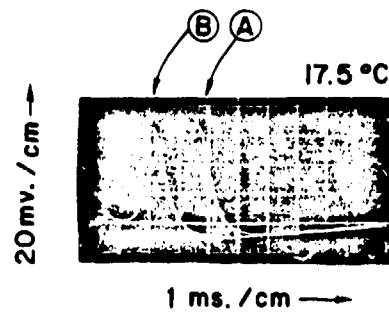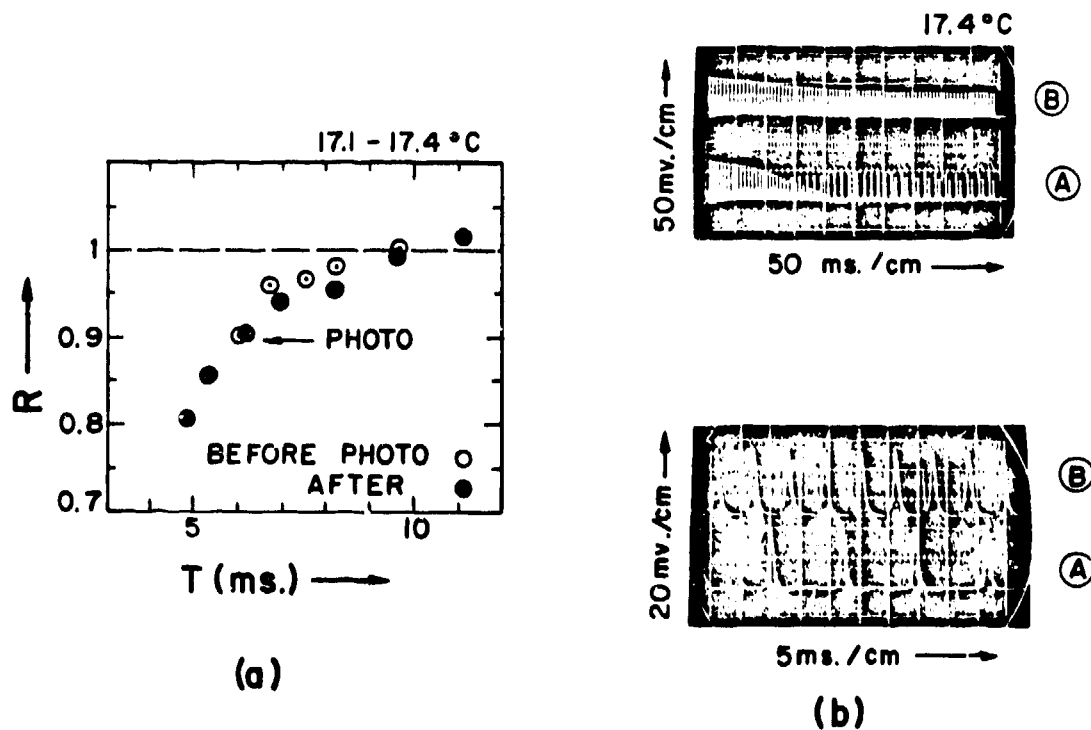
(a)

(b)

Fig. 10.  a) Bifurcation.  b) Action potentials.

(a)

(b)

Fig. 11.  a) Dispersion for bifurcation of Fig. 10.
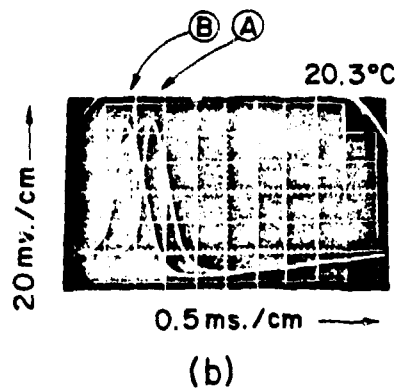b) Quantum pulse code translation after 200 ms. of stimulation.
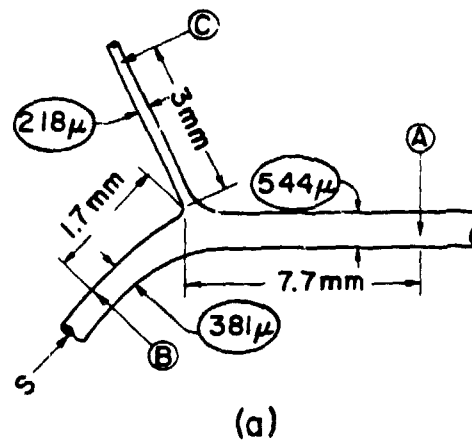
Fig. 12. a) Bifurcation. b) Action potentials.

succeeds (lower) to negotiate the bifurcation. The "hump" that appears in record (B) of the lower photo in Fig. 13 is an artifact of the appearance of the second pulse. This observation is important because it permits one to fix the position of the critical dynamic event that reproduces the second pulse. This location proceeds as follows. During the course of these experiments it was determined that conduction velocity (θ) depends upon axon diameter (d) and temperature as

$$\theta = \left[\frac{d}{476}\right]^{\frac{1}{2}} \quad [2.03 + 0.078 \ (Temp - 18.5)] \ cm/ms. \tag{8}$$

where d is measured in microns. From (10) one can calculate the time delay for a solitary pulse to go from the crotch of the bifurcation to electrode (A); this is called $T_A$. Likewise $T_B$ is calculated as the time for a pulse to travel backward from the crotch to electrode (B). The total time delay, $T_D$, between the second pulse and the hump is greater than $T_A - T_B$ because the second pulse experiences velocity dispersion as discussed in the previous section. Thus, assuming that the second pulse is triggered at the bifurcation, one expects

$$T_D = \frac{T_A - T_B}{R} \quad .$$

(9)

In Fig. 14 is displayed a comparison of time delays ($T_D$) calculated from (9) with those measured, as in Fig. 13 (lower). Agreement between measurements and calculations implies the second pulse is regenerated at the crotch of the bifurcation. The agreement in Fig. 14 indicates that the critical event took place within a millimeter of the crotch in these four cases. Since no surgical damage was observed in this region, it is reasonable to suppose that the second pulse is blocked at the bifurcation. Furthermore three of the four observations indicated in Fig. 14 show agreement with calculations of the relation between GR and pulse interval from the Hodgkin-Huxley model [30]. See [29] for details.



29 - 2 - 80 B

20.3°C

50 mv. / cm

$T_D$

0.5 ms./cm
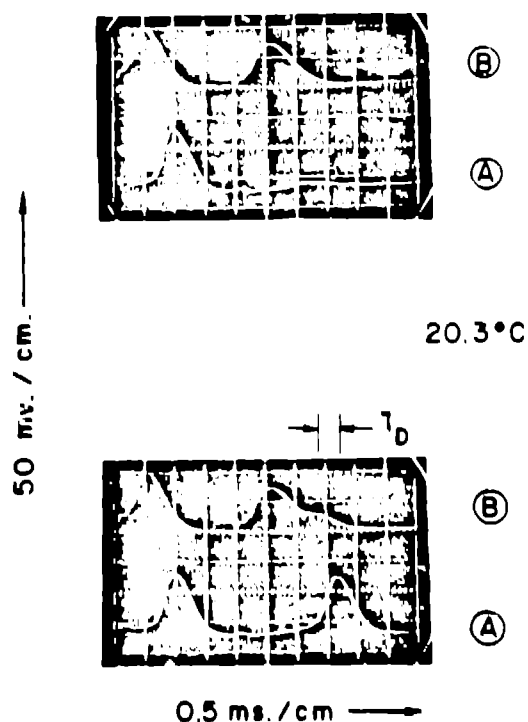
Fig. 13. The critical time interval between two pulses such that the second pulse just fails (upper) or just succeeds to pass through the branch.
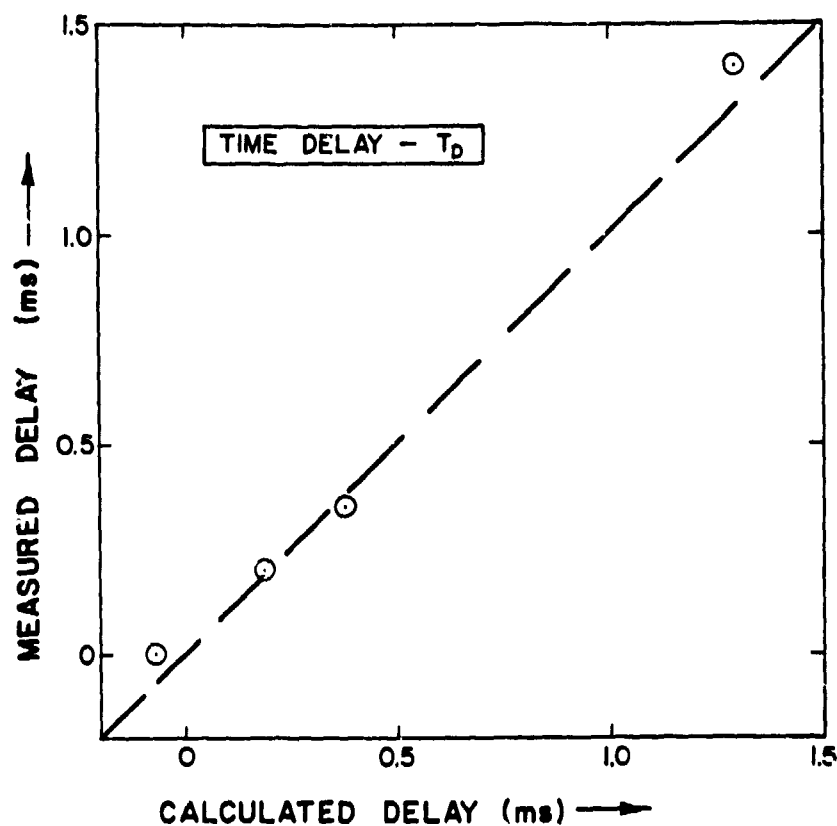
Fig. 14.   A comparison of calculated and measured time delays $(T_o)$ assuming the second is initiated at the bifurcation.

One general statement about my observations is the following:   Quantum pulse code transformations were only observed in the dispersive region where $T < T_1$ and $R < 1$.

## PULSE INTERACTIONS ON PARALLEL FIBERS

An electromagnetic analysis of two parallel fibers enclosed within an insulating sheath leads to a pair of coupled nonlinear diffusion equations [8,31-33]. In the context of a FitzHugh-Nagumo approximation [34], these take the form

$$V_{1,t} = (1 - \alpha)V_{1,xx} - \alpha V_{2,xx} - F(V_1) - R_1$$

$$R_{1,t} = \varepsilon(V_1 - bR_1)$$

$$V_{2,t} = (1 - \alpha)V_{2,xx} - \alpha V_{1,xx} - F(V_2) - R_2 \tag{10}$$

$$R_{2,t} = \varepsilon(V_2 - bR_2)$$

where the small coupling parameter is equal to the ratio of external to internal resistance per unit length. One seeks traveling wave solutions of the form

$$V_k(x,t) = V_k(\xi) = V_k(x - ut); \quad k = 1,2 \tag{11}$$

where u is the propagation speed of two pulses traveling in synchronism. Under this constraint, (10) becomes a set of ordinary differential equations

$$-u \frac{dV_1}{d\xi} = (1 - \alpha) \frac{d^2V_1}{d\xi^2} - \alpha \frac{d^2V_2}{d\xi^2} - F(V_1) - R_1$$

$$-u \frac{dR_1}{d\xi} = \varepsilon V_1$$

$$-u \frac{dV_2}{d\xi} = -\alpha \frac{d^2V_1}{d\xi^2} + (1 - \alpha) \frac{d^2V_2}{d\xi^2} - F(V_2) - R_1 \tag{12}$$

$$-u \frac{dR_2}{d\xi} = \varepsilon V_2$$

where, for convenince, it has been assumed that b = 0

A solution of (12) will be two pulses, one on each fiber, moving with the same velocity. Since $\alpha \ll 1$, this solution is written as a series

$$V_k = V_{ko} + \alpha V_{k1} + \dots ; \quad k = 1, 2$$

$$u(k) = u_o + \alpha u_1^{(k)} + \dots \tag{13}$$

where it is provisionally assumed that solutions of (12) will have different velocities for k = 1, 2. Eliminating the R's yields

$$\frac{d^3V_{ko}}{d\xi^3} + u_o \frac{d^2V_{ko}}{d\xi^2} - F'(V_{ko})\frac{dV_{ko}}{d\xi} + \frac{\varepsilon}{u_o} V_{ko} = 0 \tag{14}$$

and

$$\frac{d^3 V_{k1}}{d\xi^3} + u_o \frac{d^2 V_{k1}}{d\xi^2} - F'(V_{ko}) \frac{dV_{k1}}{d\xi} - F''(V_{ko}) \frac{dV_{ko}}{d\xi} - \frac{\varepsilon}{u}_o V$$

$$= u_1^{(k)} \frac{\varepsilon}{u_o^2} V_{ko} - \frac{d^2 V_{ko}}{d\xi^2} - \frac{d^3 V_{10}}{d\xi^3} - \frac{d^3 V_{20}}{d\xi^3} \quad . \tag{15}$$

The perturbation expanson (13) has reduced (12) to the uncoupled nonlinear equations (14) and the linear equations (15) for the first order corrections. Equations (15) are uncoupled in the $V_{k1}$ and the inhomogeneous parts involve only zero order solutions and the first order velocity perturbations. Thus each of (15) can be written

$$L_k V_{1k} = f_k \tag{15'}$$

for which a solvability condition is

$$(y_k, f_k) = 0 \tag{16}$$

where $y_k$ is a solution of

$$L_k^\dagger y_k = 0 \tag{17}$$

and $L_k^\dagger$ is the adjoint of $L_k$ un er the inner product employed in (16). With the conventional definition

$$(v,w) \equiv \int_{-\infty}^{\infty} vwd\xi$$

(17) becomes

$$\frac{d^3 y_k}{d\xi^3} - u_o \frac{d^2 y_k}{d\xi^2} - F'(V_o) \frac{dy_k}{d\xi} - \frac{\varepsilon}{u_o} y_k = 0 \tag{18}$$

From solutions of (18) one can compute inner products with the right-hand sides of (15) and obtain useful expressions for the first order velocity perturbations, the

$u_1^{(k)}$. To effect this calculation it is convenient to take

$$F(V) = V - H(V - a) \qquad (19)$$

where $H(\cdot)$ is the Heaviside step function. Choosing $a = 0.3$ and $\varepsilon = 0.1$, $V_{ko}(\xi)$ is the pulse shown in Fig. 15. Comparison with Fig. 10b or 12b shows that this choice of parameters is physiologically reasonable. The corresponding solution of (17) is shown in Fig. 16.

It is now assumed that $V_{20}$ differs from $V_{10}$ by a translation $\delta$ in $\xi$. Thus

$$V_{20}(\xi) = V_{10}(\xi - \delta)$$

$$y_2(\xi) = y_1(\xi - \delta) . \qquad (20)$$

The solvability condition (16) requires

$$Nu_1^{(k)} = - \int_{-\infty}^{\infty} y_k \left( \frac{d^3 V_{10}}{d\xi^3} + \frac{d^3 V_{20}}{d\xi^3} \right) d\xi \qquad (21)$$

where

$$N \equiv \int_{-\infty}^{\infty} y_1 \left( \frac{d^2 V_{10}}{d\xi^2} - \frac{\varepsilon}{u_o^2} V_{10} \right) d\xi = \int_{-\infty}^{\infty} y_2 \left( \frac{d^2 V_{20}}{d\xi^2} - \frac{\varepsilon}{u_o^2} V_{20} \right) d\xi . \qquad (22)$$

To first order in $\alpha$, the condition for a traveling wave solution is

$$u(1) = u_o + \alpha u_1^{(1)} = u(2) = u_o + \alpha u_1^{(2)}$$

or

$$u_1^{(1)} = u_1^{(2)} . \qquad (23)$$

In Fig. 17 these first order velocity corrections are plotted as functions of $\delta$, the displacement of pulse #2 with respect to pulse #1. Five solutions of (23) (i.e. intersections) are observed, but only three of these (at $\delta = \delta_1$, 0, and $-\delta_1$ denoted by open circles) are stable in the following sense. An increase in $\delta$
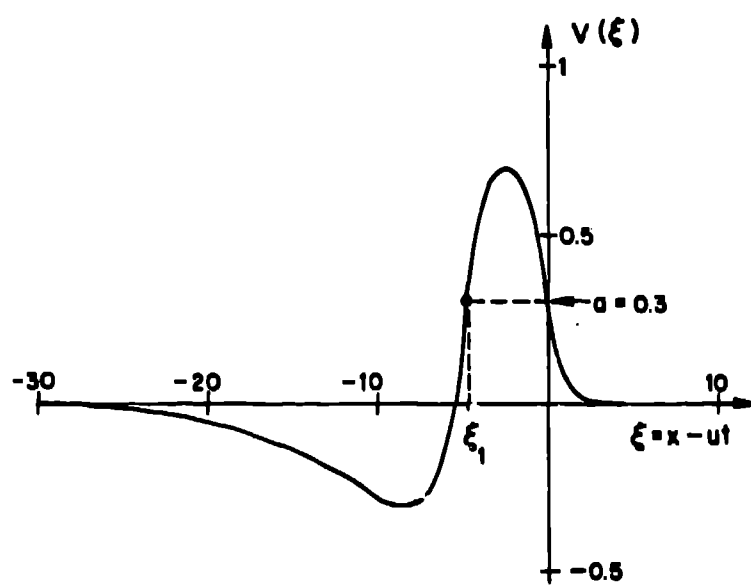
Fig. 15.  Solution of (14)
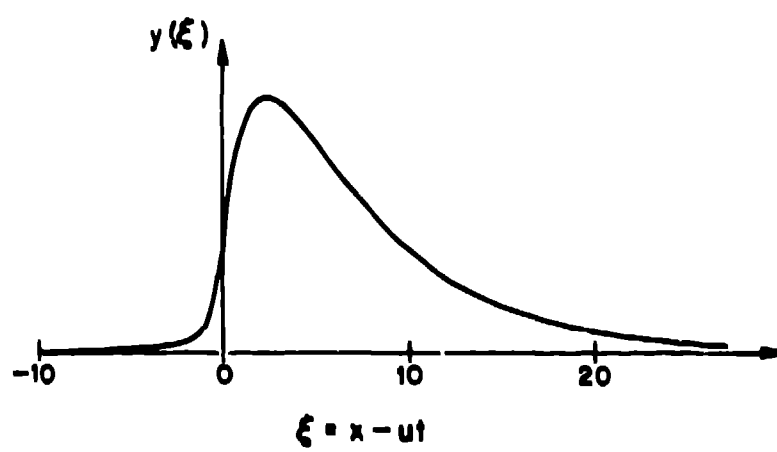


Fig. 16.  Solution of (17)

(implying that pulse #2 advances with respect to pulse #1) causes the speed of pulse #1 to become greater than that of pulse #2 which, in turn, causes $\delta$ to decrease. By a corresponding argument the intersections denoted by closed circles are unstable. This effect has been confirmed by direct integration of the original pde's (10) [35].

For n weakly coupled fibers, numbered in any order, the relative pulse displacements must satisfy the obvious constraint

$$\delta_{12} + \delta_{23} + \ldots + \delta_{n1} = 0 \quad . \tag{24}$$

For each choice of n - 1 independent $\delta$'s, one can calculate n - 1 differences of the corresponding velocity corrections as

$$D_i = u_1^{(i)} - u_1^{(i+1)}; \quad i = 1, 2, \ldots, n - 1 \quad . \tag{25}$$



Fig. 17. Stability diagram from (23).

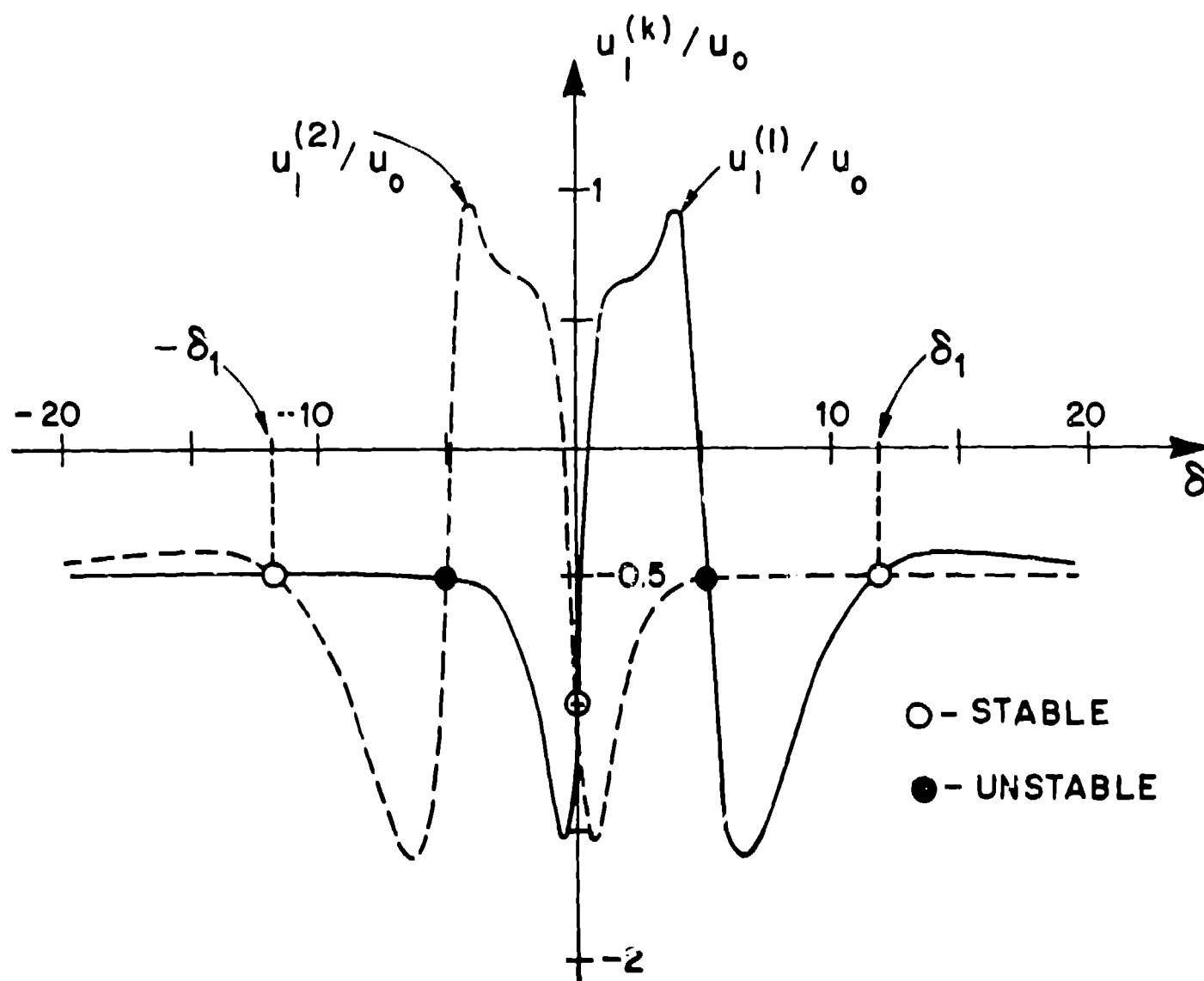Then $\bar{D} \equiv (D_1, D_2, \ldots, D_{n-1})$ is an $n - 1$ dimensional vector field in the $n - 1$ dimensional "$\delta$-space" where $\delta \equiv (\delta_{12}, \delta_{23}, \ldots, \delta_{n-1,n})$. Condensed pulse states are defined as stable zeros of

$$\bar{D} = \bar{D}(\bar{\delta}) = \bar{0} \ . \tag{26}$$

If $\delta_{i,i+1}$ denotes the position of a pulse on fiber $(i + 1)$ with respect to that of a pulse on fiber i, stability (in the sense described above) requires

$$\left. \frac{\partial D_i}{\partial \delta_{i,i+1}} \right|_{\bar{D} = \bar{0}} > 0 \tag{27}$$

for all i. For more than two coupled fibers ($n \geq 3$), this stability condition is satisfied only for the root of (26) that lies at the origin of $\delta$-space. Markin [31] has shown that if

$$\alpha n \approx 1 \tag{28}$$

this state can "recruit" additional pulses by stimulating neighboring fibers above threshold.

## THE PULSE ASSEMBLY

The recent reviews by Adey [18,19] indicate a surprising sensitivity of living tissue to nonionizing electromagnetic fields. Brain tissue, for example, responds to gradients as low as $10^{-7}$ volts/cm in the frequency range from 6 to 20 cycles per second. In speculating about mechanisms for this effect, it is necessary to consider how such weak fields can be recognized above thermal noise. More precisely one must suppose

$$\left[ \sqrt{(\pi f \mu_0 \rho)} \ E^2 \right] \cdot \sigma \geq kT\Delta f \tag{29}$$

where the square-bracketed term on the left-hand side is the power per unit area of an incident electromagnetic wave and $\sigma$ is the absorption cross-section for some (unknown) dynamical variable. On the right-hand side, $\Delta f$ is the reciprocal of the memory time for the dynamical variable. Guided by Fig. 4, one can take $\Delta f \sim T^{-1} = 100$ sec$^{-1}$. Then with $\mu_0 = 4\pi \times 10^{-7}$ henrys/meter, $\rho = 1$ ohm-meter, and $E = 10^{-7}$ volt/cm (29) implies

$$\sigma \geq 10^{-5} \text{ meter}^2$$

$$\geq (3 \text{ mm})^2 .$$

What neural mechanism could have such a large absorption cross-section? One possibility might be the "pulse assembly" sketched in Fig. 18. Here we suppose that the longitudinal pulse locking at time interval $T_1$ (see Fig. 5) is acting between pulses and D and between pulses D and E. Also we assume a transverse pulse locking, determined by (26), is acting between pulses A, B. and C and between pulses E and F.

This mechanism is highly speculative, but it would deliver information with an established time synchronism between the component pulses as is required by the information processing mechanisms that have been proposed for Waxman's multiplex neuron [16]. Furthermore it is not inconsistent with the observations of Scheibel and Scheibel [36] who have compared stained sections from newborn and mature cats and conclude that:

During the process of maturation, dendrite shafts have been found to rearrange themselves into bundles in various parts of the nervous system including the ventral horn of the spinal cord, brain stem reticular core, nucleus reticularis thalami, cerebral cortex, and possibly in basal ganglia and certain cranial nerve nuclei. In some cases, the appearance of bundle complexes seems closely time-locked to the initial development of discrete items of motor performance.
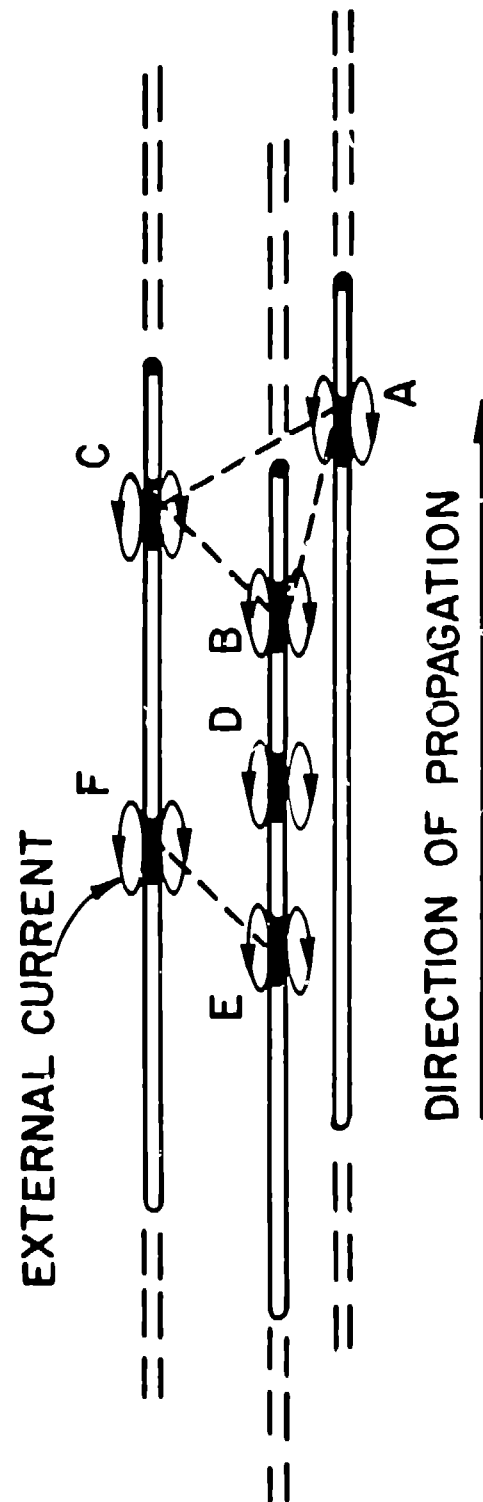
Fig. 18. Structure of a "pulse assembly."

REFERENCES

1.  R. Lorente de Nó, "Decremental conduction and summation of stimuli delivered to neurons at distant synapses," in Structure and Function of the Cerebral Cortex (Tower and Schade, eds) American Elsevier (New York, 1960) 278-281.

2.  Yu. I. Arshavskii, et al., "The role of dendrites in the functioning of nerve cells," Dokl. Akad. Nauk SSSR 163 (1965) 994-997.

3.  R. Llinás, C. Nicholson and W. Precht, "Preferred centripital conduction of dendrite spikes in alligator Purkinje cells," Sciences 163 (1969) 184-187.

4.  V. F. Pastushenko, V. S. Markin and Yu. A. Chizmadzhev, "Branching as a summator of nerve pulses," Biophysics 14 (1969) 1130-1138.

5.  A. M. Gutman, "Further remarks on the effectiveness of the dendrite synapses," Biophysics 16 (1971) 131-138.

6.  M. B. Berkinblit, et al., "Interaction of the nerve impulse in a node of branching (investigation of the Hodgkin-Huxley model)," Biophysics 16 (1971) 105-113.

7.  A. C. Scott, "Information processing in dendritic trees," Math. Biosci 18 (1973) 153-160.

8.  A. C. Scott, Neurophysics, Wiley-Interscience (New York, 1977) Ch. 6.

9.  K. Krnjević and R. Miledi, "Presynaptic failure of neuromuscular propagation in rats," J. Physiol. 149 (1959) 1-22.

10. S. H. Chung, S. A. Raymond and J. Y. Lettvin, "Multiple meaning in single visual units," Brain Behav. Evol. 3 (1970) 72-101.

11. Y. Grossman, M. E. Spira and I. Parnas, "Differential flow of information into branches of a single axon," Brain Res. 64 (1973) 379-386.

12. D. O. Smith and H. Hatt, "Axon conduction block in a region of dense connective tissue in crayfish," J. Neurophysiol. 39 (1976) 794-801.

13. Y. Grossman, I. Parnas and M. E. Spira, "Differential conduction block in branches of a bifurcating medium," J. Physiol. 295 (1979) 283-305; "Ionic mechanisms invloved in differential conduction of action potentials at high frequencies in a branching axon," ibid. 307-322.

14. D. O. Smith, "Morphological aspects of the safety factor for action potential propagation at axon branch points in the crayfish," J. Physiol. 301 (1980) 261-269; "Mechanisms of action potential propagation failure at sites of axon branching in the crayfish," ibid. 243-259.

15. F. O. Schmitt, P. Dev and B. H. Smith, "Electrotonic processing of information by brain cells," Science 193 (1976) 114-120.

16. S. G. Waxman, "Regional differentiation of the axon: a review with special reference to the concept of a multiplex neuron," Brain Res. 47 (1972) 269-288.

17. D. O. Hebb, Organization of Behavior Wiley (New York, 1949).

18. W. R. Adey, "Frequency and power windowing in tissue interactions with weak electromagnetc fields," Proc. IEEE 68 (1980) 119-125.

19. W. R. Adey, "Tissue interactions with nonionizing electromagnetic fields," Physiol. Rev. 61 (1981) 435-514

20. A. C. Scott and U. Vota-Pinardi, "Velocity variations on unmyelinated axons," J. Theoret. Neurobiol. (to appear).

21. F. Donati and H. Kunov, "A Model for studying velocity variations on unmyelinated axons," IEEE Transactions on Biomedical Engineering BME-23 (1976) 23-23.

22. R. N. Miller and J. Rinzel, "The dependence of impulse propagation speed on firing frequency, dispersion, for the Hodgkin-Huxley model," Biophys. J. 34 (1981) 227-259.

23. J. Rinzel, private communication.

24. B. Frankenhaeuser and A. L. Hodgkin, "The after-effects of impulses in the gian+ ver fibers of Loligio," J. Physiol. 131 (1956) 341-376.

25. W. .man, Jr. and R. FitzHugh, "Solutions of the Hodgkin-Huxley equations moc for potassium accumulation in a periaxonal space," Federation Proc. 34 (197, 1322-1329.

26. W. Rall, "Branching dendritic trees and motoneuron membrane resistivity," Exp. Neurol. 1 (1959) 491-527.

27. M. B. Berkinblit, et al., "Computer investigation of the features of conduction of a nerve impulse along fibers with a different degree of widening," Biophysics 15 (1970) 1121-1130.

28. I. Parnas and I. Segev, "A mathematical model for conduction of action potnetials along bifurcating axons," J. Physiol. 295 (1979) 323-343.

29. A. C. Scott and U. Vota-Pinardi, "Pulse code transformations on axonal trees," J. Theoret. Neurobiol. (to appear).

30. B. I. Khodorov. et al., "Conduction of a series of impulses through a portion of the fiber with increased diameter," Biophysics 16 (1971) 96-104.

31. V. S. Markin, "Electrical interaction of parallel nonmyelinated nerve fibers," Biophysics 15 (1970) 122-133 and 713-721; ibid. 18 (1973) 324-332 and 539-547.

32. A. C. Scott and S. D. Luzader, "Coupled solitary waves in neurophysics," Physica Scripta 20 (1979) 395-401.

33. S. D. Luzader, "Neurophysics of parallel nerve fibers," Ph.D. Thesis, University of Wisconsin (1979).

34. J. Nagumo, S. Arimoto and S. Yoshizawa, "An active pulse transmission line simulating nerve axon," Proc. IRE 50 (1962) 2061-2070.

35. J. C. Eilbeck, S. D. Luzader, A. C. Scott, "Pulse evolution on coupled nerve fibers," Bull. Math. Biol. 43 (1981) 389-400.

36. M. E. Scheibel and A. B. Scheibel, Intern. J. Neuroscience 6 (1973) 195.